Time-domain electromagnetic field transmission between small loop antennas on a half-space with conductive and dielectric properties

Stumpf, Martin; Antonini, Giulio ; Lager, Ioan E.; Vandenbosch, Guy A.E.

DOI
10.1109/TAP.2019.2943323

Publication date
2019

Document Version
Accepted author manuscript

Published in
IEEE Transactions on Antennas and Propagation

Time-Domain Electromagnetic-Field Transmission Between Small-Loop Antennas on a Half-Space With Conductive and Dielectric Properties

Martin Štumpf, *Member, IEEE*, Giulio Antonini, *Senior Member, IEEE*, Ioan E. Lager, *Senior Member, IEEE*, and Guy A. E. Vandenbosch, *Fellow, IEEE*

***Abstract*— The pulsed EM-field signal transfer between two co-planar small-loop antennas located on a half-space with dielectric and conductive properties is analyzed analytically with the help of the Cagniard–DeHoop technique and the Schouten–Van der Pol theorem. The analysis yields a closed-form time-domain expression for the open-circuit voltage induced across the ports of the receiving antenna. Limiting cases considering the mutual coupling between two loops placed in free-space and on a dielectric half-space are discussed. The obtained results are validated using analytical expressions for the special cases and with the aid of a 3-D EM computational tool.**

***Index Terms*— Cagniard–DeHoop method, electromagnetic coupling, electromagnetic propagation, electromagnetic radiation, time-domain (TD) analysis.**

I. Introduction

SINCE the early times of EM wave theory, considerable research has been devoted to the EM-field propagation along a conductive surface (see [1, Ch. VI]). In this regard, a problem of particular interest consists of a pair of small loop antennas lying on the conductive surface. This problem has been thoroughly studied in the frequency domain [2]–[6], thereby providing an efficient means for the determination of electric permittivity and conductivity of a homogeneous ground [7]. While the time-domain (TD) operation of buried loop antennas has been successfully analyzed under the quasi-static (diffusive) approximation [8], [9], the problem of loop-to-loop coupling on a lossy half-space has never been conquered analytically in the TD.

Manuscript received June 12, 2019; revised August 19, 2019; accepted September 20, 2019. Date of publication September 30, 2019; date of current version February 3, 2020. This work was supported by the Czech Ministry of Education, Youth and Sports under Grant LO1401. *(Corresponding author: Martin Štumpf.)*

M. Štumpf is with the Department of Radioelectronics, Brno University of Technology, 616 00 Brno, Czech Republic (e-mail: martin.stumpf@centrum.cz).

G. Antonini is with the UAq EMC Laboratory, University of L'Aquila, 67 100 L'Aquila, Italy (e-mail: giulio.antonini@univaq.it).

I. E. Lager is with the Faculty of Electrical Engineering, Mathematics and Computer Science, Delft University of Technology, 2628 CD Delft, The Netherlands (e-mail: i.e.lager@tudelft.nl).

G. A. E. Vandenbosch is with the Department of Electrical Engineering, Division ESAT-TELEMIC (Telecommunications and Microwaves), Katholieke Universiteit Leuven, B-3001 Leuven, Belgium (e-mail: guy.vandenbosch@esat.kuleuven.be).

Color versions of one or more of the figures in this article are available online at http://ieeexplore.ieee.org.

Digital Object Identifier 10.1109/TAP.2019.2943323

The availability of ultra-wideband pulse generators (see [10]) has enabled the development of body-centric communication systems [11], [12] and pulsed radar systems capable of probing the earth [13] or a human body [14]–[16]. Accordingly, with such TD EM applications in mind, this article aims at describing the pulsed EM-field signal transfer between two co-planar loop antennas lying on a half-space with dielectric and conductive properties. It is demonstrated that the Cagniard–DeHoop technique [17], [18] with the Schouten–Van der Pol theorem of the unilateral Laplace transformation [19], [20] is capable of meeting the goal. The analysis yields a novel closed-form TD expression for the open-circuit voltage induced across the ports of the receiving antenna. In the expression, one can clearly identify wave constituents that are propagating just above and just below the interface with the (wavefront) EM wave speeds not influenced by dispersion. In addition, a wave contribution forming the tail of the response is present. The latter contribution causes the pulse broadening and can be interpreted as a dispersion effect due to a finite half-space conductivity. Despite the latter vanishes on a dielectric half-space, the observed voltage response is still wider with respect to the exciting electric-current pulse due to the two propagation paths.

The problem configuration considered in this article is introduced in Section II. Subsequently, Section III presents the problem formulation in the TD. In virtue of the Cagniard–DeHoop technique [17], the problem is solved in Section IV in the Laplace-transform domain under the wave slowness representation. The TD solutions are provided in Section V upon invoking the results derived in the Appendices. In Section VI, the numerical results are given and validated with the aid of CST Microwave Studio®. Finally, conclusions are drawn in Section VII.

II. Problem Description

The problem configuration under consideration is shown in Fig. 1. To localize a point in the configuration, we employ the Cartesian coordinates $\{x, y, z\}$ with respect to a Cartesian reference frame with the origin $\mathcal{O}$ and the standard base $\{\boldsymbol{i}_x, \boldsymbol{i}_y, \boldsymbol{i}_z\}$. The problem configuration consists of two co-planar loop antennas $\mathcal{L}^{\mathrm{T,R}}$ lying on the interface of two semi-infinite media. The upper half-space represents the free space

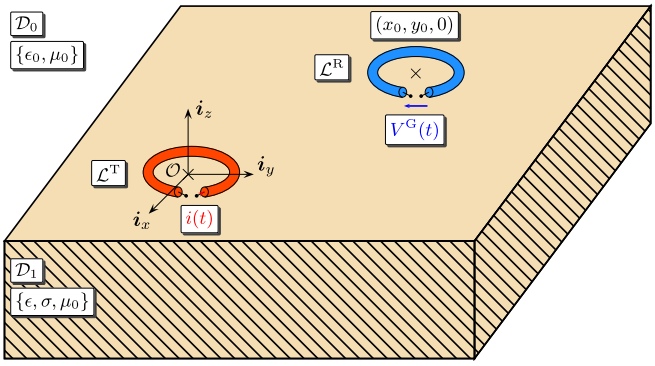

Fig. 1. Transmitting and receiving loop antennas lying on the lossy half-space.

that occupies $\mathcal{D}_0 = \{-\infty < x < \infty, -\infty < y < \infty, 0 < z < \infty\}$, while the ground extends over $\mathcal{D}_1 = \{-\infty < x < \infty, -\infty < y < \infty, -\infty < z < 0\}$. Accordingly, the EM properties of $\mathcal{D}_0$ are described by (real-valued, positive, and scalar) electric permittivity ϵ_0 and magnetic permeability μ_0, while the (homogeneous and isotropic) ground is described by its electric permittivity ϵ_1, magnetic permeability μ_0, and electric conductivity σ. The corresponding (wavefront) wave speeds in $\mathcal{D}_{0,1}$ are given by $c_{0,1} = (\epsilon_{0,1}\mu_0)^{-1/2} > 0$. The maximum diameter of the loops is assumed to be small (with respect to the spatial support of the excitation pulse) such that they can be represented by magnetic dipoles oriented along the z-axis [21, Sec. 26.10]. The transmitting antenna is, without any loss of generality, located at the origin and the receiving antenna is placed at $(x_0, y_0, 0)$ or just at $(x_0, 0, 0)$ by virtue of the circular symmetry. The areas of the transmitting and receiving loops are denoted by $\mathcal{A}^{\mathrm{T,R}}$. The time coordinate is t. The time convolution between two signals, say $f(t)$ and $g(t)$, is defined as

$$f(t) *_t g(t) = \int_{\tau=-\infty}^{\infty} f(\tau) g(t-\tau) \mathrm{d}\tau \tag{1}$$

and the time-integration operator can be then defined by

$$\partial_t^{-1} f(t) = f(t) *_t \mathrm{H}(t) = \int_{\tau=-\infty}^{t} f(\tau) \mathrm{d}\tau \tag{2}$$

where $\mathrm{H}(t)$ denotes the Heaviside-unit step function. The Dirac-delta distribution is denoted by $\delta(t)$. Finally, the partial differentiation is denoted by ∂ that is supplied with the pertaining subscript. Then, the differentiation with respect to x is denoted by ∂_x and the time derivative is denoted by ∂_t, for example.

III. Problem Formulation

Following the approach based on EM reciprocity [22], the open-circuit voltage induced at the ports of the receiving loop $\mathcal{L}^{\mathrm{R}}$ is found from

$$V^{\mathrm{G}}(t) \simeq -\mu_0 \mathcal{A}^{\mathrm{R}} \partial_t H_z^{\mathrm{e}}(x_0, y_0, 0, t) \tag{3}$$

where H_z^{e} is the z-component of the excitation (denoted by superscript e) magnetic-field strength, which corresponds to the field that would be excited by the transmitting loop in the absence of the receiving antenna. Accordingly, the magnetic field can be represented by [23, eq. (1.130)]

$$H_z^{\mathrm{e}}(x, y, z, t) = -\epsilon_0 \partial_t k(t) *_t G(x, y, z, t) + \mu_0^{-1} \partial_t^{-1} k(t) *_t \partial_z^2 G(x, y, z, t) \tag{4}$$

in $\mathcal{D}_0$ and

$$H_z^{\mathrm{e}}(x, y, z, t) = -(\epsilon_1 \partial_t + \sigma) k(t) *_t G(x, y, z, t) + \mu_0^{-1} \partial_t^{-1} k(t) *_t \partial_z^2 G(x, y, z, t) \tag{5}$$

in $\mathcal{D}_1$. Furthermore, the azimuthal component of the electric-field strength and the radial component of the magnetic-field strength can be represented with the help of [23, eqs. (1.129) and (1.130)] and [24, eqs. (A2.34) and (A2.42)] as

$$E_\phi^{\mathrm{e}}(x, y, z, t) = k(t) *_t \partial_r G(x, y, z, t) \tag{6}$$

$$H_r^{\mathrm{e}}(x, y, z, t) = \mu_0^{-1} \partial_t^{-1} k(t) *_t \partial_r \partial_z G(x, y, z, t) \tag{7}$$

respectively, in which the source signature is related to the exciting electric current $i(t)$ via [21, p. 759]

$$k(t) = \mu_0 \mathcal{A}^{\mathrm{T}} \partial_t i(t) \tag{8}$$

and G is the Green's function of the scalar wave equation applying to $\mathcal{D}_0$ and $\mathcal{D}_1$ (see [23, Sec. 2] and [21, Sec. 26.5]). With reference to (6), the continuity of E_ϕ^{e} across the interface requires

$$\lim_{z \downarrow 0} G(x, y, z, t) = \lim_{z \uparrow 0} G(x, y, z, t) \tag{9}$$

while the presence of the transmitting loop is accounted for via the excitation condition

$$\lim_{z \downarrow 0} \partial_z G(x, y, z, t) - \lim_{z \uparrow 0} \partial_z G(x, y, z, t) = -\delta(x, y)\delta(t) \tag{10}$$

for all $t > 0$ and $x \in \mathbb{R}$ and $y \in \mathbb{R}$. The thus formulated problem whose solution yields a description of the EM-field signal transfer, that is, $V^{\mathrm{G}}(t) = \mathcal{Z}(t) *_t i(t)$, is the main objective of the ensuing sections.

IV. Transform-Domain Solution

The problem will be solved with the aid of the Cagniard–DeHoop technique [17], [18] that combines a unilateral Laplace transform

$$\hat{H}_z^{\mathrm{e}}(x, y, z, s) = \int_{t=0}^{\infty} \exp(-st) H_z^{\mathrm{e}}(x, y, z, t) \mathrm{d}t \tag{11}$$

where s is the real-valued and positive transform parameter with the wave slowness representation

$$\hat{H}_z^{\mathrm{e}}(x, y, z, s) = (s/2\pi \mathrm{i})^2 \int_{\kappa=-\mathrm{i}\infty}^{\mathrm{i}\infty} \mathrm{d}\kappa \int_{\sigma=-\mathrm{i}\infty}^{\mathrm{i}\infty} \exp[-s(\kappa x + \sigma y)] \times \tilde{H}_z^{\mathrm{e}}(\kappa, \sigma, z, s) \mathrm{d}\sigma \tag{12}$$

where κ and σ are the slowness parameters in the x- and y-directions, respectively. Employing the properties $\hat{\partial}_t = s$, $\hat{\partial}_t^{-1} = 1/s$, $\tilde{\partial}_x = -s\kappa$, and $\tilde{\partial}_y = -s\sigma$, the vertical magnetic field in the transform domain follows upon using (11) and (12) in (4) and (5)

$$\tilde{H}_z^{\mathrm{e}}(\kappa, \sigma, z, s) = -s^2 \hat{i}(s) \mathcal{A}^{\mathrm{T}} (\kappa^2 + \sigma^2) \tilde{G}(\kappa, \sigma, z, s) \tag{13}$$

where the transform-domain Green's function has the following form

$$\tilde{G}(\kappa,\sigma,z,s)=\begin{cases}A\exp(-s\gamma_0 z), & \text{for } z\geq 0\\ B\exp(-s\hat{\gamma}_1 z), & \text{for } z\leq 0\end{cases} \tag{14}$$

with the vertical slowness parameters in $\mathcal{D}_{0,1}$ given by

$$\gamma_0=\left(c_0^{-2}-\kappa^2-\sigma^2\right)^{1/2} \tag{15}$$

$$\hat{\gamma}_1=\left(\hat{c}_1^{-2}-\kappa^2-\sigma^2\right)^{1/2} \tag{16}$$

respectively, with $\hat{c}_1=(c_1^{-2}+\sigma\mu_0/s)^{-1/2}>0$ and $\mathrm{Re}(\gamma_0)\geq 0$ and $\mathrm{Re}(\hat{\gamma}_1)\geq 0$. It is noted that c_1 is, in fact, the "high-frequency limit" of $\hat{c}_1$. The unknown coefficients in (14) are finally found from the interface conditions (9) and (10) in the transform domain. In this way, we obtain

$$A=B=1/(s\gamma_0+s\hat{\gamma}_1) \tag{17}$$

that fully determines the transform-domain solution. Noting the property that the transform-domain magnetic-field strength given by (13) is a function of $\kappa^2+\sigma^2$, we change the variables of integration according to

$$\kappa = p\cos(\phi)-\mathrm{i}q\sin(\phi) \tag{18}$$

$$\sigma = p\sin(\phi)+\mathrm{i}q\cos(\phi) \tag{19}$$

where $x=r\cos(\phi)$ and $y=r\sin(\phi)$ with $r=(x^2+y^2)^{1/2}>0$ and $0\leq\phi<2\pi$. Under the substitution, $\kappa x+\sigma y=pr$, $\mathrm{d}\kappa\mathrm{d}\sigma=\mathrm{i}\mathrm{d}p\mathrm{d}q$ and $\kappa^2+\sigma^2=p^2-q^2$, which implies [see (15) and (16)]

$$\gamma_0=\left[\Omega_0^2(q)-p^2\right]^{1/2} \tag{20}$$

$$\hat{\gamma}_1=\left[\hat{\Omega}_1^2(q)-p^2\right]^{1/2} \tag{21}$$

where $\Omega_0(q)=(c_0^{-2}+q^2)^{1/2}>0$ and $\hat{\Omega}_1(q)=(\hat{c}_1^{-2}+q^2)^{1/2}>0$. This finally leads to

$$\hat{H}_z^{\mathrm{e}}(x,y,z,s)=(s^2/4\pi^2\mathrm{i})\int_{q=-\infty}^{\infty}\mathrm{d}q \times\int_{p=-\mathrm{i}\infty}^{\mathrm{i}\infty}\exp(-spr)\bar{H}_z^{\mathrm{e}}(p,q,z,s)\mathrm{d}p \tag{22}$$

where $\bar{H}_z^{\mathrm{e}}(p,q,z,s)$ follows from (13) subject to the transformation (18) and (19).

V. Time-Domain Solution

Collecting the results from Section IV, the induced open-circuit voltage can be expressed as

$$\hat{V}^{\mathrm{G}}(s)\simeq\zeta_0\mathcal{A}^{\mathrm{T}}\mathcal{A}^{\mathrm{R}}s^3\hat{i}(s)\left[\hat{P}(x_0,y_0,s)-\hat{K}(x_0,y_0,s)\right] \tag{23}$$

where $\zeta_0=(\mu_0/\epsilon_0)^{1/2}$ is the wave impedance in $\mathcal{D}_0$ and the representation of functions $\hat{P}(x,y,s)$ and $\hat{K}(x,y,s)$ is discussed in Appendix A. Employing the results from the appendix, we write

$$\begin{aligned}\hat{V}^{\mathrm{G}}(s)\simeq&\left(\zeta_0\mathcal{A}^{\mathrm{T}}\mathcal{A}^{\mathrm{R}}/2\pi r_0^5\right)\hat{i}(s)\,\hat{U}(s;\alpha_0)\\&\times\{9[\exp(-sT_0)-\exp(-s\hat{T}_1)]\\&+9[sT_0\exp(-sT_0)-s\hat{T}_1\exp(-s\hat{T}_1)]\\&+4[(sT_0)^2\exp(-sT_0)-(s\hat{T}_1)^2\exp(-s\hat{T}_1)]\\&+[(sT_0)^3\exp(-sT_0)-(s\hat{T}_1)^3\exp(-s\hat{T}_1)]\}\end{aligned} \tag{24}$$

with $T_0=r_0/c_0$, $\hat{T}_1=r_0/\hat{c}_1$, $r_0=(x_0^2+y_0^2)^{1/2}>0$, and

$$\hat{U}(s;\alpha_0)=c_0/(s\chi+\alpha_0) \tag{25}$$

in which $\chi=\epsilon_1/\epsilon_0-1$ and $\alpha_0=\sigma/\epsilon_0$. The transformation of (24) back to the TD is carried out with the aid of the Schouten–Van der Pol theorem as given in Appendix B, multiple integrations by parts and some standard rules of the Laplace transformation (see [25, eq. (29.2.12)]). This way leads to the main result expressed as

$$\begin{aligned}V^{\mathrm{G}}(t)\simeq&\frac{\zeta_0\mathcal{A}^{\mathrm{T}}\mathcal{A}^{\mathrm{R}}}{2\pi r_0^2}U(t;\alpha_0)\\&*_t\left\{\left[\frac{\partial_t^3 i(t-T_0)}{c_0^3}-\frac{c_0^3}{c_1^3}\frac{\partial_t^3 i(t-T_1)}{c_0^3}\exp(-\alpha_1T_1/2)\right]\right.\\&+\frac{4}{r_0}\left[\frac{\partial_t^2 i(t-T_0)}{c_0^2}-\frac{c_0^2}{c_1^2}\left(1-\frac{3}{8}\alpha_1T_1+\frac{1}{32}\alpha_1^2T_1^2\right)\right.\\&\left.\times\frac{\partial_t^2 i(t-T_1)}{c_0^2}\exp(-\alpha_1T_1/2)\right]\\&+\frac{9}{r_0^2}\left[\frac{\partial_t i(t-T_0)}{c_0}-\frac{c_0}{c_1}\left(1-\frac{4}{9}\alpha_1T_1+\frac{7}{72}\alpha_1^2T_1^2\right.\right.\\&\left.-\frac{1}{72}\alpha_1^3T_1^3+\frac{1}{1152}\alpha_1^4T_1^4\right)\frac{\partial_t i(t-T_1)}{c_0}\exp(-\alpha_1T_1/2)\Big]\\&+\frac{9}{r_0^3}\left[i(t-T_0)-\left(1-\frac{1}{2}\alpha_1T_1+\frac{1}{8}\alpha_1^2T_1^2-\frac{1}{48}\alpha_1^3T_1^3\right.\right.\\&+\frac{1}{384}\alpha_1^4T_1^4-\frac{1}{2304}\alpha_1^5T_1^5+\frac{1}{27648}\alpha_1^6T_1^6\Big)\\&\left.\left.\times i(t-T_1)\exp(-\alpha_1T_1/2)\right]\right\}+V_0^{\mathrm{G}}(t)\end{aligned} \tag{26}$$

where $\alpha_1=\sigma/\epsilon_1$ and [see (25)]

$$U(t;\alpha_0)=(c_0/\chi)\exp(-\alpha_0t/\chi)\mathrm{H}(t) \tag{27}$$

and

$$\begin{aligned}V_0^{\mathrm{G}}(t)=&\frac{\zeta_0\mathcal{A}^{\mathrm{T}}\mathcal{A}^{\mathrm{R}}}{2\pi r_0^5}\frac{\alpha_1}{2}\,i(t)*_tU(t;\alpha_0)\\&*_t\big[9\,\Gamma(t,\tau;\alpha_1)|_{\tau=T_1}-9\,T_1\partial_\tau\Gamma(t,\tau;\alpha_1)|_{\tau=T_1}\\&+4\,(T_1)^2\partial_\tau^2\Gamma(t,\tau;\alpha_1)|_{\tau=T_1}-(T_1)^3\\&\times\partial_\tau^3\Gamma(t,\tau;\alpha_1)|_{\tau=T_1}\big]\\&\times\exp(-\alpha_1\,t/2)\mathrm{H}(t-T_1)\end{aligned} \tag{28}$$

with

$$\Gamma(t,\tau;\alpha)=\frac{\tau}{(t^2-\tau^2)^{1/2}}\mathrm{I}_1[(\alpha/2)(t^2-\tau^2)^{1/2}] \tag{29}$$

where $\mathrm{I}_1(x)$ denotes the modified Bessel function of the first kind and first order. The differentiations of (29) with respect to τ readily follow and can be found in Appendix C.

The voltage response described by (26) consists of wave constituents that are proportional to (a weighted sum of) the exciting current and its first, second, and third time derivatives. Clearly, the wave constituents appear at the receiving loop at the (wavefront) arrival times $T_{0,1}=r_0/c_{0,1}=r_0(\epsilon_{0,1}\mu_0)^{1/2}$

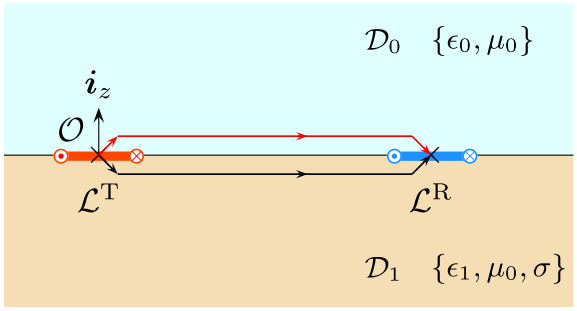

Fig. 2. Ray trajectories of the wave constituents.

corresponding to $\mathcal{D}_{0,1}$ that are not affected by the electric conductivity of the lower half-space (see Fig. 2). Accordingly, these arrival times have been previously associated with forerunners propagating along a conductive surface [26]. The TD analytical solution represented by (26) further reveals that the wave constituents propagating in the conductive half-space undergo the exponential decay whose rate is proportional to the inverse of the relaxation time $\epsilon_1/\sigma = 1/\alpha_1$ and distance r_0. Owing to the exponential damping, the latter constituents can be for good conductors essentially neglected with respect to the ones traveling above the interface. In fact, before the disturbance propagating at wavefront speed $c_1 = (\epsilon_1\mu_0)^{-1/2}$ appears, the wave constituents associated with the free-space travel time T_0 are the only non-vanishing constituents, thus forming the early time part of the voltage response. Consequently, referring to (26), we may write

$$V^{\mathrm{G}}(t) \simeq \frac{\zeta_0 \mathcal{A}^{\mathrm{T}}\mathcal{A}^{\mathrm{R}}}{2\pi r_0^2} U(t;\alpha_0) *_t \left[\frac{\partial_t^3 i(t-T_0)}{c_0^3} + \frac{4}{r_0}\frac{\partial_t^2 i(t-T_0)}{c_0^2} + \frac{9}{r_0^2}\frac{\partial_t i(t-T_0)}{c_0} + \frac{9}{r_0^3} i(t-T_0) \right] \tag{30}$$

for $\{0 \le t < T_1\}$, without introducing any further approximation. The remaining term $V_0^{\mathrm{G}}(t)$ in (26) does not contribute to the initial part of the response and can be, hence, interpreted as a relaxational effect shaping the long-time tail of the induced voltage signal.

The existence of forerunners has been first theoretically predicted by Sommerfeld [27, Ch. II and III] who analyzed 1-D wave propagation through a dispersive medium. His solution based on a time Fourier-integral representation consists of two very weak forerunners followed by a dominant wave packet traveling with the so-called group velocity. While the first forerunner observed in the dispersive medium propagates at the speed of light much like the initial disturbance described by (30), the latter is not subject to drastic exponential damping.

For a lossless half-space, $\alpha_{0,1} = 0$ and (26) boils down to

$$\lim_{\sigma \downarrow 0} V^{\mathrm{G}}(t) \simeq \frac{\zeta_0 \mathcal{A}^{\mathrm{T}}\mathcal{A}^{\mathrm{R}}}{2\pi r_0^2} U(t;0) *_t \left\{ \left[\frac{\partial_t^3 i(t-T_0)}{c_0^3} - \frac{c_0^3}{c_1^3}\frac{\partial_t^3 i(t-T_1)}{c_0^3} \right] + \frac{4}{r_0}\left[\frac{\partial_t^2 i(t-T_0)}{c_0^2} - \frac{c_0^2}{c_1^2}\frac{\partial_t^2 i(t-T_1)}{c_0^2} \right] + \frac{9}{r_0^2}\left[\frac{\partial_t i(t-T_0)}{c_0} - \frac{c_0}{c_1}\frac{\partial_t i(t-T_1)}{c_0} \right] + \frac{9}{r_0^3}\left[i(t-T_0) - i(t-T_1) \right] \right\} \tag{31}$$

Since $U(t;0)$, in fact, represents the scaled Heaviside step function, the time convolution in (31) can be carried out analytically and we end up with

$$\lim_{\sigma \downarrow 0} V^{\mathrm{G}}(t) \simeq \frac{\zeta_0 \mathcal{A}^{\mathrm{T}}\mathcal{A}^{\mathrm{R}}}{2\pi r_0^2}\frac{1}{\chi} \times \left\{ \left[\frac{\partial_t^2 i(t-T_0)}{c_0^2} - \frac{c_0^3}{c_1^3}\frac{\partial_t^2 i(t-T_1)}{c_0^2} \right] + \frac{4}{r_0}\left[\frac{\partial_t i(t-T_0)}{c_0} - \frac{c_0^2}{c_1^2}\frac{\partial_t i(t-T_1)}{c_0} \right] + \frac{9}{r_0^2}\left[i(t-T_0) - (c_0/c_1) i(t-T_1) \right] + \frac{9}{r_0^3}\left[c_0\partial_t^{-1} i(t-T_0) - c_0\partial_t^{-1} i(t-T_1) \right] \right\} \tag{32}$$

and recall that $\chi = \epsilon_1/\epsilon_0 - 1$. Finally, if $\mathcal{D}_1$ does not show any EM contrast with respect to the upper half-space $\mathcal{D}_0$, we get a well-known expression for the "Thévenin equivalent generator voltage"

$$\lim_{\chi \downarrow 0}\lim_{\sigma \downarrow 0} V^{\mathrm{G}}(t) \simeq \frac{\zeta_0 \mathcal{A}^{\mathrm{T}}\mathcal{A}^{\mathrm{R}}}{4\pi r_0} \left\{ \frac{\partial_t^3 i(t-T_0)}{c_0^3} + \frac{1}{r_0}\frac{\partial_t^2 i(t-T_0)}{c_0^2} + \frac{1}{r_0^2}\frac{\partial_t i(t-T_0)}{c_0} \right\} \tag{33}$$

which is consistent with (the TD counterpart of) (23) with the limit (45) and with the results introduced in [22] and [28].

VI. Illustrative Numerical Examples

We shall evaluate the pulsed EM transfer between two co-planar loop antennas lying on the surface of a dielectric/conductive half-space. The loops have the shape of a square whose sides have a length $a = 50$ mm and areas $\mathcal{A}^{\mathrm{T}} = \mathcal{A}^{\mathrm{R}} = a^2$. The receiving loop is located at $(x_0, y_0) = (2.0, 1.0)$ m with respect to the center of the transmitter (see Fig. 1) so that the distance between the antennas is $r_0 = \sqrt{5}$ m. The transmitting loop is excited by a causal electric-current pulse with finite temporal support that can be simply constructed by convolving two triangular pulses, that is,

$$i(t) = \frac{16 i_{\mathrm{m}}}{3}\left[\left(\frac{t}{t_{\mathrm{w}}}\right)^3 \mathrm{H}(t) - 2\left(\frac{t}{t_{\mathrm{w}}} - \frac{1}{4}\right)^3 \mathrm{H}\left(\frac{t}{t_{\mathrm{w}}} - \frac{1}{4}\right) + 2\left(\frac{t}{t_{\mathrm{w}}} - \frac{3}{4}\right)^3 \mathrm{H}\left(\frac{t}{t_{\mathrm{w}}} - \frac{3}{4}\right) - 2\left(\frac{t}{t_{\mathrm{w}}} - 1\right)^3 \mathrm{H}\left(\frac{t}{t_{\mathrm{w}}} - 1\right) \right.$$

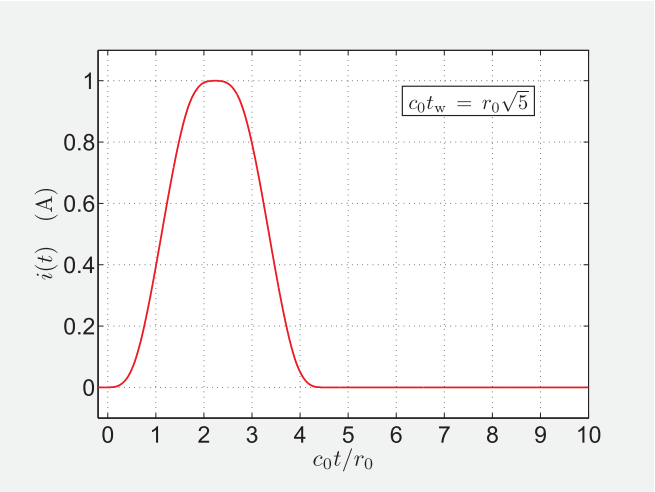

Fig. 3. Excitation electric-current pulse shape.

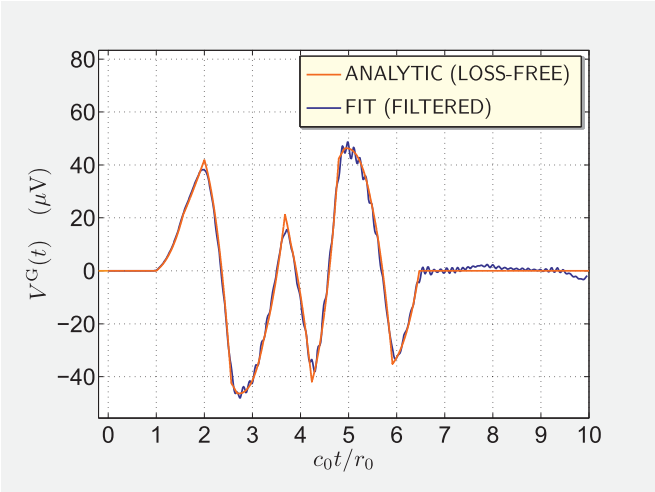

Fig. 4. Open-circuit voltage induced in the receiving loop on the loss-free dielectric half-space with $\epsilon_1 = 4.0\epsilon_0$.

$$+2\left(\frac{t}{t_w}-\frac{5}{4}\right)^3 \mathrm{H}\left(\frac{t}{t_w}-\frac{5}{4}\right)-2\left(\frac{t}{t_w}-\frac{7}{4}\right)^3 \mathrm{H}\left(\frac{t}{t_w}-\frac{7}{4}\right) + \left(\frac{t}{t_w}-2\right)^3 \mathrm{H}\left(\frac{t}{t_w}-2\right)\Bigg] \tag{34}$$

with the unit amplitude $i_m = 1.0$ A and the spatial support of the pulse described by $c_0 t_w / r_0 = \sqrt{5}$ (see Fig. 3). Consequently, $c_0 t_w = 100a$ so that the loops are relatively small as assumed before. For validation purposes, the induced voltages will also be calculated with the aid of the finite-integration technique (FIT) as implemented in CST Microwave Studio®. The computational CST-FIT model consists of a "brick" with defined dielectric/conductive properties whose side lengths are 10 m × 10 m × 5.0 m, along the x-, y-, and z-directions, respectively. The transmitting antenna that is composed of four "discrete ports" forming the square loop is placed on the top of the brick. The resulting pulses representing the z-component of the excitation magnetic-field strength are recorded using a standard "H-field probe" located at the interface of the brick and the surrounding space at distance r_0 from the center of the source. The induced voltage is subsequently calculated according to (3) in a post-processing procedure. Around the analyzed structure, we prescribe the standard "open (add space)" boundary conditions. The model is spatially discretized into mesh cells such that the parameter (maximum mesh step)/$c_0 t_w$ is always less than 1/40.

In the first example, the antennas are placed on a loss-free dielectric half-space whose permittivity is $\epsilon_1 = 4.0\epsilon_0$. Fig. 4 shows that the resulting voltage responses as calculated using (32) and FIT agree well. As the response calculated via FIT suffered from fast oscillations whose period was neither related to the characteristic travel times within the analyzed problem configuration nor to reflections from its outer boundary, we easily removed the artifacts using a simple 3-point moving average filter [29, Sec. 6.4.1]. As the total voltage response is composed of wave constituents propagating at the front wave speed c_0 and of slower ones propagating at $c_1 = c_0/2$, its pulse time width is, despite the dispersion-free half-space, greater than the one of the exciting electric current (see Fig. 3).

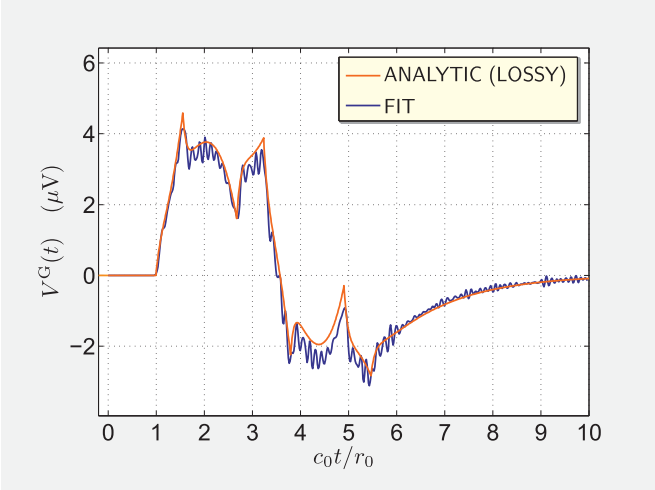

Fig. 5. Open-circuit voltage induced in the receiving loop on the lossy half-space with $\epsilon_1 = 4.0\epsilon_0$ and $\sigma = 50$ mS/m.

In the second case, the lower half-space is described by $\epsilon_1 = 4.0\epsilon_0$, again, and by a non-vanishing electric conductivity $\sigma = 50$ mS/m (see [30, Sec. III.B]). Fig. 5 shows the corresponding pulse shapes calculated using (26) and FIT, again. Apparently, the received voltage pulse is highly attenuated with respect to the one shown in Fig. 4. On top of this, the finite conductivity has a significant impact on the pulse shape as well as on the pulse time width.

In order to further reveal the impact of the conductivity on the induced voltage waveform, we next apply a narrower excitation pulse with $c_0 t_w = 50a$ so that the spatial extent of the pulse in $\mathcal{D}_0$ is approximately equal to the distance between the antennas, namely, $c_0 t_w / r_0 = \sqrt{5}/2 \simeq 1.12$.

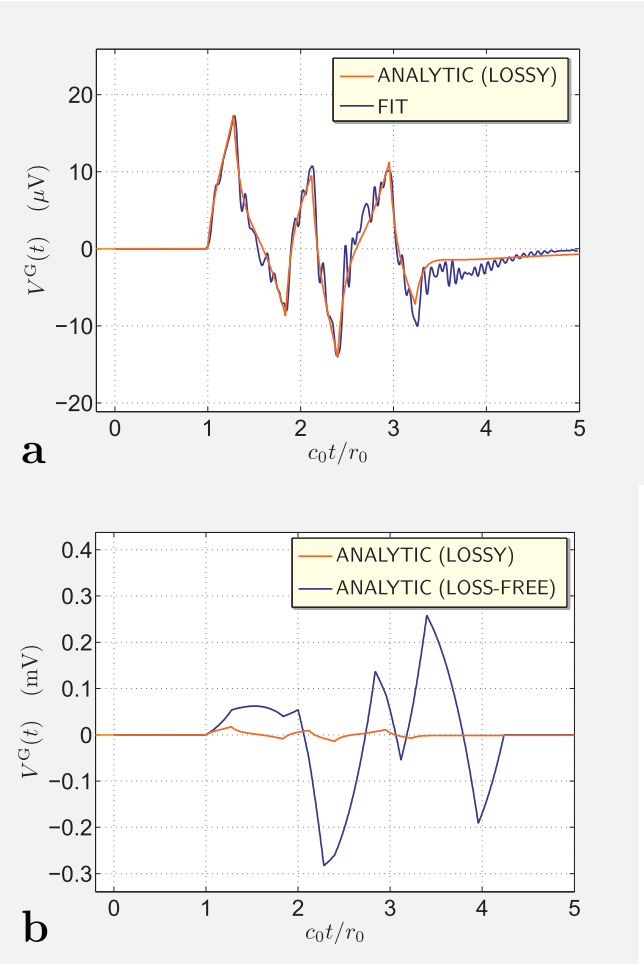

Fig. 6. (a) Open-circuit voltage due to a relatively short electric-current pulse with $c_0t_w = 50a$ as induced at the receiving loop on the lossy half-space with $\epsilon_1 = 4.0\epsilon_0$ and $\sigma = 50$ mS/m. (b) Comparison with the corresponding result observed on the dielectric half-space with $\epsilon_1 = 4.0\epsilon_0$ and $\sigma = 0$.

Fig. 6(a) then shows the open-circuit voltage response as calculated via (26) and using FIT, while in Fig. 6(b), we compare the response with the corresponding one pertaining to the loss-free dielectric half-space. It is clearly seen that the response just after $t = T_0$ (i.e., $c_0t/r_0 = 1$) is much less affected by the finite conductivity then the later part after $t = T_1$ (i.e., $c_0t/r_0 = 2$). This observation is attributed to the fact that the wave constituents whose ray trajectory goes through (lossy) $\mathcal{D}_1$ (see Fig. 2) are highly attenuated, which is not the case for the (loss-free) dielectric half-space. This observation is also compatible with a frequency-domain view that dispersive phenomena are imperceptible at observation times close to the initial wavefront (with its high-frequency content) and manifest themselves later when low-frequency constituents become important [31].

VII. Conclusion

The pulsed EM signal transmission between two co-planar loop antennas located on a lossy half-space was described analytically via the Cagniard–DeHoop technique and the Schouten–Van der Pol theorem. A closed-form space-time expression for the open-voltage induced in the receiving antenna was introduced and discussed. It follows that the resulting voltage response can be constructed from a weighted sum of the exciting current and its first, second, and third time derivatives and from a late-time tail due to a finite conductivity. Numerical examples illustrated special features of the space-time solution that are not directly apparent from the available frequency-domain results. The analytical formulas are suitable for validation and benchmarking of purely numerical techniques. It is further anticipated that the introduced methodology is applicable to describing the EM pulse transmission between buried antennas, which is commonly analyzed with the aid of general-purpose direct-discretization techniques (see [30]) at the expense of high computational demands.

Appendix

A. Generic Integrals

In this appendix, the slowness-domain representations of constitutive functions $\hat{P}(x, y, s)$ and $\hat{K}(x, y, s)$ [see (23)] are cast into a form that is amenable to inversion to the TD.

1) Representation of Function $\hat{P}(x, y, s)$: The slowness representation of the constitutive function $\hat{P}(x, y, s)$ is given by

$$\hat{P}(x, y, s) = \frac{s}{4\pi^2 \mathrm{i}} \frac{c_0^{-1}}{\hat{c}_1^{-2} - c_0^{-2}} \int_{q=-\infty}^{\infty} \mathrm{d}q \times \int_{p=-\mathrm{i}\infty}^{\mathrm{i}\infty} \exp(-spr)\hat{\gamma}_1(p, q)(p^2 - q^2)\mathrm{d}p \quad (35)$$

for $r > 0$ and $s > 0$ with $\hat{\gamma}_1$ given by (21). The integration contour along the imaginary axis in the complex p-plane is further deformed into the loop encircling the branch cut $\{0 < \hat{\Omega}_1(q) < \mathrm{Re}(p) < \infty, \mathrm{Im}(p) = 0\}$. The deformation is permissible since $sr > 0$, thus getting a vanishingly small integrand along supplementing circular arcs of infinite radius in $\mathrm{Re}(p) > 0$. The loop is associated with the Cagniard–DeHoop path, say $\mathcal{C} \cup \mathcal{C}^*$, with

$$\mathcal{C} = \{p(\tau) = \tau/r + \mathrm{i}0\} \quad (36)$$

for $\{\tau \in \mathbb{R}; r\hat{\Omega}_1(q) \leq \tau < \infty\}$. Combining the contributions from $\mathcal{C}$ and $\mathcal{C}^*$ and introducing τ as the new variable of integration, we get

$$\hat{P}(x, y, s) = -\frac{s}{2\pi^2 r^2} \frac{c_0^{-1}}{\hat{c}_1^{-2} - c_0^{-2}} \int_{q=-\infty}^{\infty} \mathrm{d}q \int_{\tau=r\hat{\Omega}_1(q)}^{\infty} \exp(-s\tau) \times [p^2(\tau) - q^2]\left[\tau^2 - r^2\hat{\Omega}_1^2(q)\right]^{1/2}\mathrm{d}\tau \quad (37)$$

In the next step, we change the order of the integrations and use the fact that the integrand is an even function of q. We then obtain

$$\hat{P}(x, y, s) = -\frac{s}{\pi^2 r} \frac{c_0^{-1}}{\hat{c}_1^{-2} - c_0^{-2}} \int_{\tau=\hat{D}_1}^{\infty} \exp(-s\tau)\mathrm{d}\tau \times \int_{q=0}^{\hat{Q}_1(\tau)} [\tau^2/r^2 - q^2]\left[\hat{Q}_1^2(\tau) - q^2\right]^{1/2}\mathrm{d}q \quad (38)$$

where $\hat{Q}_1(\tau) = (\tau^2/r^2 - \hat{c}_1^{-2})^{1/2}$ and $\hat{D}_1 = r/\hat{c}_1$. The integral with respect to q can be carried out analytically, which yields

$$\begin{aligned}\hat{P}(x,y,s) = &-\frac{sc_0^{-1}}{16\pi r}\frac{c_0^2/\hat{c}_1^2}{c_0^2-\hat{c}_1^2}\frac{3}{\hat{D}_1^4}\int_{\tau=\hat{D}_1}^{\infty}\exp(-s\tau)\tau^4\mathrm{d}\tau\\ &+\frac{sc_0^{-1}}{16\pi r}\frac{c_0^2/\hat{c}_1^2}{c_0^2-\hat{c}_1^2}\frac{2}{\hat{D}_1^2}\int_{\tau=\hat{D}_1}^{\infty}\exp(-s\tau)\tau^2\mathrm{d}\tau\\ &+\frac{sc_0^{-1}}{16\pi r}\frac{c_0^2/\hat{c}_1^2}{c_0^2-\hat{c}_1^2}\int_{\tau=\hat{D}_1}^{\infty}\exp(-s\tau)\mathrm{d}\tau \qquad (39)\end{aligned}$$

which is a sum of Laplace-transform integrals [see (11)].

2) Representation of Function $\hat{K}(x,y,s)$: The slowness representation of the constitutive function $\hat{K}(x,y,s)$ is given by

$$\begin{aligned}\hat{K}(x,y,s) = &\frac{s}{4\pi^2\mathrm{i}}\frac{c_0^{-1}}{\hat{c}_1^{-2}-c_0^{-2}}\int_{q=-\infty}^{\infty}\mathrm{d}q\\ &\times\int_{p=-\mathrm{i}\infty}^{\mathrm{i}\infty}\exp(-spr)\gamma_0(p,q)(p^2-q^2)\mathrm{d}p \qquad (40)\end{aligned}$$

for $r > 0$ and $s > 0$ with γ_0 given by (20). Following the lines of reasoning from Section VII, the integration contour is first replaced with the corresponding Cagniard–DeHoop path, say $\mathcal{G}\cup\mathcal{G}^*$, whose parametrization is

$$\mathcal{G} = \{p(\tau) = \tau/r + \mathrm{i}0\} \qquad (41)$$

for $\{\tau\in\mathbb{R}; r\Omega_0(q)\le\tau<\infty\}$ [see (20)]. Again, introducing τ as the new variable of integration, combining the contributions from $\mathcal{G}$ and $\mathcal{G}^*$, and changing the order of the integrations with respect to q and τ, we end up with [see (38)]

$$\begin{aligned}\hat{K}(x,y,s) = &-\frac{s}{\pi^2 r}\frac{c_0^{-1}}{\hat{c}_1^{-2}-c_0^{-2}}\int_{\tau=D_0}^{\infty}\exp(-s\tau)\mathrm{d}\tau\\ &\times\int_{q=0}^{Q_0(\tau)}[\tau^2/r^2-q^2]\big[Q_0^2(\tau)-q^2\big]^{1/2}\mathrm{d}q \qquad (42)\end{aligned}$$

where $\hat{Q}_0(\tau) = (\tau^2/r^2 - c_0^{-2})^{1/2}$ and $D_0 = r/c_0$. Evaluating the inner integral, we get

$$\begin{aligned}\hat{K}(x,y,s) = &-\frac{sc_0^{-1}}{16\pi r}\frac{\hat{c}_1^2/c_0^2}{c_0^2-\hat{c}_1^2}\frac{3}{D_0^4}\int_{\tau=D_0}^{\infty}\exp(-s\tau)\tau^4\mathrm{d}\tau\\ &+\frac{sc_0^{-1}}{16\pi r}\frac{\hat{c}_1^2/c_0^2}{c_0^2-\hat{c}_1^2}\frac{2}{D_0^2}\int_{\tau=D_0}^{\infty}\exp(-s\tau)\tau^2\mathrm{d}\tau\\ &+\frac{sc_0^{-1}}{16\pi r}\frac{\hat{c}_1^2/c_0^2}{c_0^2-\hat{c}_1^2}\int_{\tau=D_0}^{\infty}\exp(-s\tau)\mathrm{d}\tau \qquad (43)\end{aligned}$$

which has, again, the form of Laplace-transform integrals.

3) Difference $\hat{P}(x,y,s) - \hat{K}(x,y,s)$: With reference to (23), we shall evaluate the difference of (39) and (43). To that end, the integrations with respect to τ are carried out analytically and we end up with

$$\begin{aligned}&\hat{P}(x,y,s)-\hat{K}(x,y,s)\\ &= \frac{1}{2\pi r}\frac{c_0^{-1}}{c_0^2-\hat{c}_1^2}\left[\frac{\hat{c}_1^2}{c_0^2}\frac{\exp(-sD_0)}{sD_0}-\frac{c_0^2}{\hat{c}_1^2}\frac{\exp(-s\hat{D}_1)}{s\hat{D}_1}\right]\\ &\quad+\frac{4}{2\pi r}\frac{c_0^{-1}}{c_0^2-\hat{c}_1^2}\left[\frac{\hat{c}_1^2}{c_0^2}\frac{\exp(-sD_0)}{s^2D_0^2}-\frac{c_0^2}{\hat{c}_1^2}\frac{\exp(-s\hat{D}_1)}{s^2\hat{D}_1^2}\right]\\ &\quad+\frac{9}{2\pi r}\frac{c_0^{-1}}{c_0^2-\hat{c}_1^2}\left[\frac{\hat{c}_1^2}{c_0^2}\frac{\exp(-sD_0)}{s^3D_0^3}-\frac{c_0^2}{\hat{c}_1^2}\frac{\exp(-s\hat{D}_1)}{s^3\hat{D}_1^3}\right]\\ &\quad+\frac{9}{2\pi r}\frac{c_0^{-1}}{c_0^2-\hat{c}_1^2}\left[\frac{\hat{c}_1^2}{c_0^2}\frac{\exp(-sD_0)}{s^4D_0^4}-\frac{c_0^2}{\hat{c}_1^2}\frac{\exp(-s\hat{D}_1)}{s^4\hat{D}_1^4}\right]. \qquad (44)\end{aligned}$$

It is interesting to observe that the following limit

$$\begin{aligned}&\lim_{\hat{c}_1\uparrow c_0}[\hat{P}(x,y,s)-\hat{K}(x,y,s)]\\ &\qquad=\frac{1}{4\pi r}\frac{1}{c_0^3}\left[1+\frac{1}{sD_0}+\frac{1}{s^2D_0^2}\right]\exp(-sD_0) \qquad (45)\end{aligned}$$

when used in (23) conforms with the description of a two-loop EM-field transfer system [22, Sec. IX]. Equation (44) has been used in (23) to find the closed-form expression (24) for the open-circuit voltage response in the s-domain.

B. Schouten–Van der Pol Theorem for the Replacement of s by $(s^2-\alpha^2/4)^{1/2}$

Let $f(t)$ be a causal function whose Laplace transform is

$$\hat{f}(s) = \int_{\tau=0}^{\infty}\exp(-s\tau)f(\tau)\mathrm{d}\tau \qquad (46)$$

for $\{s\in\mathbb{R}; s>0\}$. Consequently, replacing s with $(s^2-\alpha^2/4)^{1/2}$ leads to

$$\begin{aligned}\hat{F}(s;\alpha) &= \hat{f}[(s^2-\alpha^2/4)^{1/2}]\\ &= \int_{\tau=0}^{\infty}\exp[-(s^2-\alpha^2/4)^{1/2}\tau]f(\tau)\mathrm{d}\tau. \qquad (47)\end{aligned}$$

The TD counterpart of the latter is found with the aid of

$$\exp[-(s^2-\alpha^2/4)^{1/2}\tau] = \int_{t=0}^{\infty}\exp(-st)\Omega(t,\tau;\alpha)\mathrm{d}t \qquad (48)$$

where (see [25, eq. (29.3.96)])

$$\begin{aligned}\Omega(t,\tau;\alpha) = &\delta(t-\tau)+(\alpha/2)\tau(t^2-\tau^2)^{-1/2}\\ &\times\mathrm{I}_1[(\alpha/2)(t^2-\tau^2)^{1/2}]\mathrm{H}(t-\tau). \qquad (49)\end{aligned}$$

Substituting (48) in (47) and using Lerch's uniqueness theorem [32, Appendix], we arrive at

$$\begin{aligned}F(t;\alpha) = f(t)+(\alpha/2)\int_{\tau=0}^{t}f(\tau)\mathrm{I}_1[(\alpha/2)(t^2-\tau^2)^{1/2}]\\ \times\frac{\tau\,\mathrm{d}\tau}{(t^2-\tau^2)^{1/2}}. \qquad (50)\end{aligned}$$

Equation (50) will be used to find the TD voltage response (26).

C. Supplementing Expressions

The differentiations of (29) can be carried out analytically, which yields

$$\begin{aligned}\partial_\tau\Gamma(t,\tau;\alpha) = &\frac{t^2+\tau^2}{t^2-\tau^2}\frac{\mathrm{I}_1[(\alpha/2)(t^2-\tau^2)^{1/2}]}{(t^2-\tau^2)^{1/2}}\\ &-\frac{\alpha\tau}{2}\frac{\tau}{(t^2-\tau^2)^{1/2}}\frac{\mathrm{I}_0[(\alpha/2)(t^2-\tau^2)^{1/2}]}{(t^2-\tau^2)^{1/2}} \qquad (51)\\ \partial_\tau^2\Gamma(t,\tau;\alpha)] = &\left[\frac{6\tau}{(t^2-\tau^2)^{1/2}}+\frac{8\tau^3}{(t^2-\tau^2)^{3/2}}\right.\end{aligned}$$

$$+\frac{\alpha^2\tau^2}{4}\frac{\tau}{(t^2-\tau^2)^{1/2}}\Bigg]\frac{\mathrm{I}_1[(\alpha/2)(t^2-\tau^2)^{1/2}]}{t^2-\tau^2} - \alpha\tau\left[\frac{2\tau^2}{t^2-\tau^2}+\frac{3}{2}\right]\frac{\mathrm{I}_0[(\alpha/2)(t^2-\tau^2)^{1/2}]}{t^2-\tau^2} \tag{52}$$

and finally

$$\partial_\tau^3\Gamma(t,\tau;\alpha) = \left[6+\frac{3\alpha^2\tau^2}{2}+\frac{48\tau^2}{t^2-\tau^2}+\frac{48\tau^4}{(t^2-\tau^2)^2} + 2\alpha^2\tau^2\frac{\tau^2}{t^2-\tau^2}\right]\frac{\mathrm{I}_1[(\alpha/2)(t^2-\tau^2)^{1/2}]}{(t^2-\tau^2)^{3/2}} - \left[\tfrac{3}{2}\alpha(t^2-\tau^2)^{1/2}+12\alpha\tau\frac{\tau}{(t^2-\tau^2)^{1/2}} + 12\alpha\tau\frac{\tau^3}{(t^2-\tau^2)^{3/2}}+\frac{\alpha^3\tau^3}{8}\frac{\tau}{(t^2-\tau^2)^{1/2}}\right] \times \frac{\mathrm{I}_0[(\alpha/2)(t^2-\tau^2)^{1/2}]}{(t^2-\tau^2)^{3/2}}. \tag{53}$$

Expressions (29) with (51)–(53) can be used in (28) to calculate the time convolution with $U(t;\alpha_0)$. In this respect, it is noted that $\Gamma(t,\tau;\alpha)$ and its derivatives are bounded as $t\to\tau$. Indeed, the limits of (51)–(53) read

$$\lim_{t\to\tau}\Gamma(t,\tau;\alpha) = \frac{1}{4}\alpha\tau \tag{54}$$

$$\lim_{t\to\tau}\partial_\tau\Gamma(t,\tau;\alpha) = \alpha\left(\frac{1}{4}-\frac{1}{64}\alpha^2\tau^2\right) \tag{55}$$

$$\lim_{t\to\tau}\partial_\tau^2\Gamma(t,\tau;\alpha) = -\alpha^2\left(\frac{3}{64}\alpha\tau-\frac{1}{1536}\alpha^3\tau^3\right) \tag{56}$$

$$\lim_{t\to\tau}\partial_\tau^3\Gamma(t,\tau;\alpha) = -\alpha^3\left(\frac{3}{64}-\frac{1}{256}\alpha^2\tau^2+\frac{1}{49152}\alpha^4\tau^4\right) \tag{57}$$

respectively. Notwithstanding the bounded limits, the evaluation of the time-convolution integrals in (28) is a challenging task. Accordingly, nearly singular integrals can be evaluated via stretching the variable of integration [33, Sec. VIII].

ACKNOWLEDGMENT

The authors would like to extend their thanks to the (anonymous) reviewers for their careful reading of the article and their constructive suggestions for the improvement of this article. The research reported in this article was carried out during a visiting professorship M. Štumpf had effectuated at the UAq EMC Laboratory, University of L'Aquila, Italy.

REFERENCES

[1] A. Sommerfeld, *Partial Differential Equations in Physics*. New York, NY, USA: Academic, 1949.
[2] J. R. Wait, "Current-carrying wire loops in a simple inhomogeneous region," *J. Appl. Phys.*, vol. 23, no. 4, pp. 497–498, 1952.
[3] J. R. Wait, "Mutual electromagnetic coupling of loops over a homogeneous ground," *Geophysics*, vol. 20, no. 3, pp. 630–637, 1955.
[4] M. Parise, "Exact electromagnetic field excited by a vertical magnetic dipole on the surface of a lossy half-space," *Prog. Electromagn. Res.*, vol. 23, pp. 69–82, 2010.
[5] M. Parise, M. Muzi, and G. Antonini, "Loop antennas with uniform current in close proximity to the earth: Canonical solution to the surface-to-surface propagation problem," *Prog. Electromagn. Res.*, vol. 77, pp. 57–69, 2017.
[6] J. Nagar, B. Q. Lu, M. F. Pantoja, and D. H. Werner, "Analytical expressions for the mutual coupling of loop antennas valid from the RF to optical regimes," *IEEE Trans. Antennas Propag.*, vol. 65, no. 12, pp. 6889–6903, Dec. 2017.
[7] J. R. Wait, "Mutual coupling of loops lying on the ground," *Geophysics*, vol. 19, no. 2, pp. 290–296, 1954.
[8] J. R. Wait and D. A. Hill, "Transient signals from a buried magnetic dipole," *J. Appl. Phys.*, vol. 42, no. 10, pp. 3866–3869, 1971.
[9] J. R. Wait and D. A. Hill, "Transient electromagnetic fields of a finite circular loop in the presence of a conducting half-space," *J. Appl. Phys.*, vol. 43, no. 11, pp. 4532–4534, 1972.
[10] F. Zito, D. Pepe, and D. Zito, "UWB CMOS monocycle pulse generator," *IEEE Trans. Circuits Syst. I, Reg. Papers*, vol. 57, no. 10, pp. 2654–2664, May 2010.
[11] S. L. Cotton, "A statistical model for shadowed body-centric communications channels: Theory and validation," *IEEE Trans. Antennas Propag.*, vol. 62, no. 2, pp. 1416–1424, Mar. 2014.
[12] L. A. Y. Poffelie, P. J. Soh, S. Yan, and G. A. E. Vandenbosch, "A high-fidelity all-textile UWB antenna with low back radiation for off-body WBAN applications," *IEEE Trans. Antennas Propag.*, vol. 64, no. 2, pp. 757–760, Feb. 2016.
[13] S. Vitebskiy, L. Carin, M. A. Ressler, and F. H. Le, "Ultra-wideband, short-pulse ground-penetrating radar: Simulation and measurement," *IEEE Trans. Geosci. Remote Sens.*, vol. 35, no. 3, pp. 762–772, May 1997.
[14] F. Thiel and F. Seifert, "Noninvasive probing of the human body with electromagnetic pulses: Modeling of the signal path," *J. Appl. Phys.*, vol. 105, no. 4, 2009, Art. no. 044904.
[15] Ø. Aardal, Y. Paichard, S. Brovoll, T. Berger, T. S. Lande, and S.-E. Hamran, "Physical working principles of medical radar," *IEEE Trans. Biomed. Eng.*, vol. 60, no. 4, pp. 1142–1149, Apr. 2013.
[16] H. Song *et al.*, "Detectability of breast tumor by a hand-held impulse-radar detector: Performance evaluation and pilot clinical study," *Sci. Rep.*, vol. 7, no. 1, 2017, Art. no. 16353.
[17] A. T. De Hoop, "A modification of Cagniard's method for solving seismic pulse problems," *Appl. Sci. Res.*, vol. 8, no. 1, pp. 349–356, 1960.
[18] M. Štumpf, A. T. De Hoop, and G. A. E. Vandenbosch, "Generalized ray theory for time-domain electromagnetic fields in horizontally layered media," *IEEE Trans. Antennas Propag.*, vol. 61, no. 5, pp. 2676–2687, May 2013.
[19] J. P. Schouten, "A new theorem in operational calculus together with an application of it," *Physica*, vol. 2, nos. 1–12, pp. 75–80, 1935.
[20] B. van der Pol, "A theorem on electrical networks with an application to filters," *Physica*, vol. 1, pp. 521–530, May 1934.
[21] A. T. de Hoop, *Handbook of Radiation and Scattering of Waves*. London, U.K.: Academic, 1995.
[22] A. T. De Hoop, I. E. Lager, and V. Tomassetti, "The pulsed-field multiport antenna system reciprocity relation and its applications—A time-domain approach," *IEEE Trans. Antennas Propag.*, vol. 57, no. 3, pp. 594–605, Mar. 2009.
[23] S. H. Ward and G. W. Hohmann, "Electromagnetic theory for geophysical applications," *Electromagn. Methods Appl. Geophys.*, vol. 1, no. 3, pp. 130–311, 1988.
[24] J. G. van Bladel, *Electromagnetic Fields*, 2nd ed. Hoboken, NJ, USA: Wiley, 2007.
[25] M. Abramowitz and I. A. Stegun, *Handbook of Mathematical Functions*. New York, NY, USA: Dover, 1972.
[26] G. J. Weir, "Forerunners on conducting surfaces: The infinitesimal vertical magnetic dipole with displacement terms," *Geophys. J. Int.*, vol. 81, no. 1, pp. 19–31, 1985.
[27] L. Brillouin, *Wave Propagation and Group Velocity*. New York, NY, USA: Academic, 1960.
[28] I. E. Lager and A. T. de Hoop, "Loop-to-loop pulsed electromagnetic field wireless signal transfer," in *Proc. 6th Eur. Conf. Antennas Propag.*, 2012, pp. 786–790.
[29] A. V. Oppenheim, *Signals Systems*, 2nd ed. Upper Saddle River, NJ, USA: Prentice-Hall, 1997.
[30] A. S. Kesar and E. Weiss, "Wave propagation between buried antennas," *IEEE Trans. Antennas Propag.*, vol. 61, no. 12, pp. 6152–6156, Nov. 2013.
[31] L. B. Felsen, "Propagation and diffraction of transient fields in non-dispersive and dispersive media," in *Transient Electromagnetic Fields*. New York, NY, USA: Springer-Verlag, 1976, pp. 1–72.

[32] M. Štumpf, *Electromagnetic Reciprocity in Antenna Theory*. Hoboken, NJ, USA: Wiley, 2018.
[33] A. T. D. Hoop, M. Štumpf, and I. E. Lager, "Pulsed electromagnetic field radiation from a wide slot antenna with a dielectric layer," *IEEE Trans. Antennas Propag.*, vol. 59, no. 8, pp. 2789–2798, Aug. 2011.

Martin Štumpf (M'15) received the Ph.D. degree in electrical engineering from the Brno University of Technology (BUT), Brno, Czech Republic, in 2011.

He was a Post-Doctoral Fellow with the ESAT-TELEMIC Division, Katholieke Universiteit Leuven, Leuven, Belgium. During a 3-month period in 2018, he was a Visiting Professor with the UAq EMC Laboratory, University of L'Aquila, L'Aquila, Italy. He is currently an Associate Professor with the Department of Radioelectronics, BUT. He has authored the books titled *Electromagnetic Reciprocity in Antenna Theory* (Wiley–IEEE Press, 2017), *Pulsed EM Field Computation in Planar Circuits: The Contour Integral Method* (CRC Press, 2018), and *Time-Domain Electromagnetic Reciprocity in Antenna Modeling* (Wiley–IEEE Press, 2019). His current research interest includes modeling of electromagnetic wave phenomena with an emphasis on EMC and antenna engineering.

Giulio Antonini (M'94–SM'05) received the Laurea degree *(cum laude)* in electrical engineering from the University of L'Aquila, L'Aquila, Italy, in 1994, and the Ph.D. degree in electrical engineering from the University of Rome "La Sapienza," Rome, Italy, in 1998.

Since 1998, he has been with the UAq EMC Laboratory, University of L'Aquila, where he is currently a Professor. He has coauthored the book *Circuit Oriented Electromagnetic Modeling Using the PEEC Techniques* (Wiley–IEEE Press, 2017). His current research interest includes computational electromagnetics.

Ioan E. Lager (SM'14) received the M.Sc. degree from the "Transilvania" University of Braşov, Braşov, Romania, in 1987, the Ph.D. degree from the Delft University of Technology, Delft, The Netherlands, in 1996, and the Ph.D. degree from the "Transilvania" University of Braşov, in 1998, all in electrical engineering.

He successively occupied several research and academic positions with the "Transilvania" University of Braşov and the Delft University of Technology, where he is currently an Associate Professor. In 1997, he was a Visiting Scientist with the Schlumberger-Doll Research, Ridgefield, CT, USA. He has a special interest for bridging the gap between electromagnetic field theory and the design, implementation, and physical measurement of radio frequency front-end architectures. His research interests include applied electromagnetics, especially time-domain propagation and applications, and antenna engineering, with an emphasis on nonperiodic (interleaved) array antenna architectures. He currently investigates effective methods for teaching electromagnetic field theory at (under)graduate-level.

Guy A. E. Vandenbosch (M'92–SM'08–F'13) received the M.S. and Ph.D. degrees in electrical engineering from Katholieke Universiteit Leuven, Leuven, Belgium, in 1985 and 1991, respectively.

From 1991 to 1993, he held a post-doctoral research position at the Katholieke Universiteit Leuven. Since 1993, he has been a Lecturer, and a Full Professor with the Katholieke Universiteit Leuven since 2005. He has taught or teaches courses on "Electromagnetic Waves," "Antennas," "Electromagnetic Compatibility," "Electrical Engineering, Electronics, and Electrical Energy," and "Digital Steer and Measuring Techniques in Physics." His work has been published in ca. 310 articles in international journals and has led to ca. 375 articles at international conferences. His current research interests include electromagnetic theory, computational electromagnetics, planar antennas and circuits, nanoelectromagnetics, EM radiation, EMC, and bioelectromagnetics.

Dr. Vandenbosch has been a member of the "Management Committees" of the consecutive European COST actions on antennas since 1993. From 2008 to 2014, he was a member of the board of FITCE Belgium, the Belgian branch of the Federation of Telecommunications Engineers of the European Union. Within the ACE Network of Excellence of the EU from 2004 to 2007, he was a member of the Executive Board and coordinated the activity on the creation of a European antenna software platform. He currently leads the EuRAAP Working Group on Software and represents this group within the EuRAAP Delegate Assembly. From 2001 to 2007, he was the President of SITEL, the Belgian Society of Engineers in Telecommunication and Electronics. From 1999 to 2004, he was the Vice-Chairman, from 2005 to 2009, a Secretary, and from 2010 to 2017, the Chairman of the IEEE Benelux Chapter on Antennas en Propagation. From 2002 to 2004, he was a Secretary of the IEEE Benelux Chapter on EMC. From 2012 to 2014, he was a Secretary of the Belgian National Committee for Radio-Electricity (URSI), where he is also in charge of commission E. From September to December 2014, he was a Visiting Professor with Tsinghua University, Beijing, China.